The dynamics of binary mixtures of nonpolymeric viscoelastic liquids as studied by quasielastic light scattering

B. Gerharz, G. Meier, and E. W. Fischer

Citation: The Journal of Chemical Physics **92**, 7110 (1990); doi: 10.1063/1.458251
View online: http://dx.doi.org/10.1063/1.458251
View Table of Contents: http://scitation.aip.org/content/aip/journal/jcp/92/12?ver=pdfcov
Published by the AIP Publishing

The dynamics of binary mixtures of nonpolymeric viscoelastic liquids as studied by quasielastic light scattering

B. Gerharz, G. Meier, and E. W. Fischer
Max-Planck-Institut für Polymerforschung, D-6500 Mainz, Federal Republic of Germany

(Received 8 January 1990; accepted 27 February 1990)

In this paper we report quasielastic light-scattering experiments of the compatible binary mixture of simple viscoelastic liquids made up of *o*-terphenyl as one component and newly synthesized model materials, 1,1-di(paramethoxyphenyl)-cyclo-hexan and 1,1-di(paramethoxyphenyl, metamethyl)-cyclohexan, as the other components. The measurements were done in a wide temperature range above T_g ($\simeq T_g + 100$ K) of the mixtures and in a volume fraction range up to $\phi = 0, 5$ of bis-cresol-cyclohexane-dimethylether and bis-phenol-cyclohexane-dimethylether. We have found that the measured dynamics is governed by three effects: At short times we observe the dynamics of the density fluctuations of the system characterized by a broad distribution of relaxation times, which can be scaled to a masterplot taking the T_g of the mixtures into account. At longer times we observe two translational diffusion processes whose decay is single exponential with a characteristic time proportional to q^{-2}, q being the scattering vector. The faster one is attributed to the interdiffusion coefficient of the system. The second, slower mode is related to the motion of dynamic clusters which have their origin in a spatial inhomogeneity of the samples. The mean cluster diameter is about 1000 Å, thus in any case the occurrence of the slow mode is accompanied by a strong increase of the elastically scattered intensity towards small scattering angles. This mode also appears in pure components. We relate its intensity to the fluctuations of an order parameter, usually introduced to describe the glassy state.

I. INTRODUCTION

Light scattering from binary mixtures as studied by photon correlation spectroscopy has gained tremendous importance, especially in the dilute region of macromolecules in solution,[1] and has been widely used to characterize polymer properties. This field is, as commonly believed, well understood. However, very concentrated solutions are not understood and studied to that extent.[2] One can realize a concentrated solution simply by mixing two kinds of molecules of almost similar mass, and then study its dynamics at elevated temperatures over a wide concentration range as was successfully done in the case of binary polymer blends.[3,4] In this case the dynamics of concentration fluctuations were analyzed to give the mutual diffusion coefficient, which describes the motion of one component relative to the other. The objective of those papers was to find out which theoretical model is applicable for combining the microscopic Rouse mobilities of the individual species to give the measured diffusivity. In order to allow the proper determination of the diffusion coefficient, the mixtures have to be measured at temperatures high enough such that the center of mass translates, in a typical time window of the photon correlation experiment ($10^{-6} < t < 10^{2}$ s.), over a distance q^{-1} where q is the scattering vector in a light-scattering experiment (typically 10^{-3} Å^{-1}). This of course determines the range of accessible diffusion coefficients typically in the range of 10^{-4}–10^{-12} cm^2/s. For example, for poly(styrene) (PS) (one of the components used in the mixture studies reported in Ref. 3) the diffusion coefficient has a value of 5×10^{-9} cm^2/s at T = 150 °C which is roughly 100 K above the glass transition temperature T_g of the PS used in the study.[5] On the other hand, the dynamics of density fluctuations for this material at the same temperature difference to T_g is almost in the GHz region.[6] However, the question of interest is whether and how many transport processes will appear if the system is approaching its glass transition temperature. The polymer mixture PS/poly(methylphenysiloxane) (PMPS)[3] has an upper critical solution temperature T_c, but for the chosen molecular weights the T_g(mix) is lower than T_c. Thus the possible influence of the critical dynamics, approaching the glass transition temperature, on the mutual diffusion coefficient could not be studied. In the literature only very few hints towards this problem exist, where usually the concentration and density fluctuations are assumed to be independent and light scattering from binary mixtures can be used to measure thermodynamical quantities like activity coefficients[7] or the free-energy function.[8] A considerable interdependence of both fluctuations was predicted only for components having low molecular weight using a molecular model[9] and was verified experimentally.[10] A recent publication also predicts a coupling[11] of density variables (internal degrees of freedom) to slowly relaxing concentration fluctuations (critical fluctuations).

The main problem, however, is the experimental verification, as it is extremely difficult to measure the dynamics of both density and concentration fluctuations by means of photon correlation spectroscopy within the accessible time window of the experiment. The first experiment showing such a case was performed by Fytas *et al.*,[12] where they studied the relaxation processes in PMPS contaminated with its own oligomer. But due to the great dynamic separation of

0021-9606/90/127110-13$03.00

density and concentration fluctuations the complete activation plot could only be obtained by performing high-pressure experiments leading to a substantial slowing down of the density fluctuations.[13] The unwanted use of an additional parameter to characterize the different relaxation modes can only be overcome by a proper choice of systems. The first attempt was undertaken recently by Floudas, Fytas, and Ngai,[14] who examined poly(cyclohexylmethacrylate) (PCHMA) plasticized with up to 15% dioctylphatalate (DOP), and were able to measure density and concentration fluctuations. Furthermore, the use of polymer mixtures is not appropriate because of the great dynamic separation of both effects. We decided to investigate mixtures of nonpolymeric glass-forming liquids where the dynamics of density fluctuations is accessible, and furthermore we can access the diffusional process because of the high viscosity of the systems when approaching T_g. The systems used were mixtures of *o*-terphenyl (OTP) with two related tailormade new glass-forming systems bis-phenol-cyclohexane-dimethylether (BCDE) and bis-cresol-cyclohexane-dimethylether (BKDE):

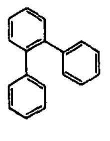

OTP

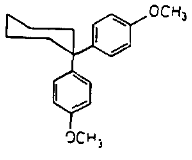

BCDE*

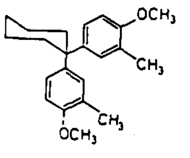

BKDE**

*[1,1-Di(paramethoxyphenyl)-cyclohexan]
**[1,1-Di(paramethoxyphenyl,metamethyl)-cyclohexan]

The concentration ranges used were up to a volume fraction of $\phi = 0.5$. In the course of this research we have not only encountered density and concentration fluctuations, but also a long-time slow process which already has given rise to many speculations in the literature. So far, this seems to be a characteristic feature for highly concentrated systems where at least one component is of polymeric nature.[2,15–17] Furthermore, a slow mode in charged, concentrated systems was also observed,[18] as well as in binary melts of polymers.[19,20] We have found this feature in our nonpolymeric mixtures but with enhanced intensity. Based upon the comparison between our results obtained for the mixtures and for the pure components,[21] we propose a model for the slow mode which relates the excess intensity, characterizing the slow mode, to the fluctuations of an order parameter $z(P,T)$, known to describe the glassy state. A combination of angular-dependent dynamic and static light scattering was used to further characterize this process. Additionally, kinetic experiments to influence the occurrence and stability of the clusters giving rise to the slow process were performed in order to study the dependence of this process on the thermal history of the sample.

II. THEORY: LIGHT SCATTERING AND THERMODYNAMICS

Considering the case of light scattering from binary mixtures, we follow the general route given in Kerker's book.[22] There the fluctuations in the dielectric constant are written as

$$\delta\epsilon = \left[\frac{\partial\epsilon}{\partial\rho}\right]_{T,m}\delta\rho + \left[\frac{\partial\epsilon}{\partial T}\right]_{\rho,m}\delta T + \left[\frac{\partial\epsilon}{\partial m}\right]_{\rho,T}\delta m, \qquad (1)$$

where ρ is the density and m is the "molality" expressed in mass of component one over the mass of component two. Usually for a liquid the second term is assumed to be small and is therefore neglected. In a first approximation density and concentration fluctuations defined in the foregoing way[23] are not correlated, and by taking the square of $\delta\epsilon$ and averaging, the averages of the cross terms reduce to zero, and result in

$$\langle\delta\epsilon^2\rangle = \left[\frac{\partial\epsilon}{\partial\rho}\right]^2_{T,m}\langle\delta\rho^2\rangle + \left[\frac{\partial\epsilon}{\partial m}\right]^2_{\rho,T}\langle\delta m^2\rangle. \qquad (2)$$

This leads to two terms for the scattered intensity, one arising from density fluctuations, the other one from concentration fluctuations. The averaged quadratic fluctuation of ρ can be related to the isothermal compressibility β_T of the system,[23]

$$\lim_{q\to 0}\langle\delta\rho^2\rangle = (1/V)\rho^2 k_B T\beta_T. \qquad (3)$$

The term $[\partial\epsilon/\partial\rho]^2$ gives the amplitude factor for the fluctuation term. Thus $[\partial\epsilon/\partial\rho]^2_T\langle\delta\rho^2\rangle$ is related to the total scattered intensity I_D due to density fluctuations at $q = 0$. Using the Clausius–Mossotti equation, one can, in general, calculate the quantity $[\partial\epsilon/\partial\rho]_T$ and hence estimate I_D. It has been found experimentally that the scattered intensity I_D calculated by Eq. (3) with a known $\partial\epsilon/\partial\rho$ does not describe the experimental features, but it is almost 2 orders of magnitude lower.[24] We have further investigated a similar excess scattering in pure OTP (Ref. 21) and pure BKDE (unpublished results). There we have introduced the scattering order parameter $z(P,T)$ which depends also on thermal history. The use of such an order parameter is usually used to describe scattering in the glassy state.[25] Hence, we assume phenomenologically an equation derived in analogy to scattering from concentration fluctuations to be valid for this excess scattering,

$$I_{\mathrm{ex}} = \left[\frac{\partial\epsilon}{\partial z}\right]^2\langle\delta z^2\rangle. \qquad (4)$$

Thus we have to modify Eq. (2) to account for the total scattered intensity,

$$\langle\delta\epsilon^2\rangle = \left[\frac{\partial\epsilon}{\partial\rho}\right]_{T,m,z}\langle\delta\rho^2\rangle + \left[\frac{\partial\epsilon}{\partial m}\right]_{\rho,T,z}\langle\delta m^2\rangle + \left[\frac{\partial\epsilon}{\partial z}\right]^2_{T,\rho,m}\langle\delta z^2\rangle. \qquad (5)$$

Hence when we perform a dynamic experiment in doing quasielastic light scattering, we are interested in the time dependence of $\delta\rho$ entering Eq. (2). The quantity $\langle\delta\rho(\mathbf{q},t)\delta\rho(\mathbf{q},0)\rangle$ is directly connected with $I_D(\mathbf{q},t)$.[1] Then the measurement of $\langle I(\mathbf{q},t)I(\mathbf{q},0)\rangle$ allows us to calculate $g(\mathbf{q},t)$ by using Eq. (12). Further, we connect the time-dependent intensity with dynamic mechanical properties, recalling the result from the Wang–Fischer theory,[26] which relates the time autocorrelation function of density fluctuations to the time-dependent longitudinal compliance via

$$\alpha g(\mathbf{q},t) = \frac{\beta_T - D(t)}{\beta_s}, \tag{6}$$

where α is further defined in Eq. (12), β_s is the adiabatic compressibility, and $D(t)$ the transient longitudinal compliance. The latter quantity can in most cases be substituted by $B(t)$, the time-dependent bulk compliance.[27] The objective to relate the light-scattering spectrum to dynamic mechanical properties is to point out the applicability of the time temperature (frequency) superposition principle which we will use to construct master curves for the measured density autocorrelation functions. The use of the latter principle was shown to be valid for polymeric systems when measuring the dynamics of the α relaxation with photon correlation spectroscopy.[28]

Now we consider the second term in Eq. (5) dealing with concentration fluctuations. The general equation to describe the scattering from concentration fluctuations of a miscible two-component system covering the whole concentration range is conveniently given by[22]

$$I_c = KVk_BTx_1 \left[\frac{\partial \mu_2}{\partial x_2}\right]^{-1}_{T,p}, \tag{7}$$

where $K = 2\pi^2 n^2 [\partial n/\partial x_i]^2/\lambda^4$ and V is the molar volume of the solution. The other symbols have the usual meaning. The concentrations are expressed in mole fraction x. For the relation of x to the "molality," defined in Eq. (1), the reader is referred to Davidson's book.[23] To relate the measured intensity to an absolute intensity, one usually introduces the Rayleigh factor R^{c}_{vv}, where c stands for the concentration fluctuation of the interdiffusion process, via

$$R^{c}_{vv} = \left[\frac{I_c}{I_{\text{benzene}}}\right] \left[\frac{n_{\text{solution}}}{n_{\text{benzene}}}\right]^2 R^{\text{benzene}}_{vv}. \tag{8}$$

We used R^{benzene}_{vv} for a scattering angle of $\theta = 90°$, $T = 25$ °C, and $\lambda_0 = 488$ nm being $R^{\text{benzene}}_{vv} = 3.66 \times 10^{-5}\ \text{cm}^{-1}$.[29]

For an ideal solution the equation

$$\mu_i - \mu_i^0 = R \cdot T \cdot \ln x_i \tag{9}$$

is valid. Introducing this expression into Eq. (7), we get the expression

$$I_c^{\text{id}} = KVx_1x_2 \tag{10}$$

for the ideal concentration fluctuation.

To summarize briefly, at this point we have three scattering contributions [cf. Eq. (5)] of which only the one due to concentration fluctuations can be calculated from basic thermodynamical formulas [cf. Eq. (10)]. Obviously, Eq. (2) does not properly describe all the scattering processes; therefore, we have to introduce additional excess scattering [Eq. (5)].

III. EXPERIMENTAL METHODS

A. Measurements of T_g

The glass transition temperatures T_g of the pure materials and of the mixtures were determined by differential scanning calorimetry (DSC) at different heating rates t_R such that a heating-rate independent T_g was achieved by extrapolation to $t_R \to 0$. In Fig. 1 the results of the measurements are shown. The glass transition temperatures of the mixtures BCDE/OTP behave according to the Kelley–Bueche equation[30] with a K value of zero, whereas for BKDE/OTP mixtures $K \neq 0$, and hence formally an additional "excess T_g" effect can be noticed.

B. Measurements of viscosity

We have measured the steady flow (shear) viscosity η_s of the pure components and for two mixtures BCDE/OTP with $x_1 = 0.3$ and BKDE/OTP with $x_1 = 0.5$ by means of a Rheometrix torsion pendulum. The viscosity is calculated by

$$\eta_s = \lim_{\omega \to 0} \frac{G''(\omega)}{\omega}.$$

To achieve this, frequency-dependent measurements of the shear modulus $G''(\omega)$ have to be extrapolated to $\omega \to 0$ after reaching a constant plateau value. Usually the temperature dependence of η_s can be described by the Vogel–Fulcher–Tammann (VFT) equation:

$$\eta_s(T) = \eta_0 \exp\left(\frac{B}{T - T_\infty}\right), \tag{11}$$

where η_0, B, and T_∞ are treated as fit parameters. We have listed the resulting values in Table I together with the values of T_g obtained from DSC measurements, and have plotted the data in Fig. 2. Using the fit parameters from Eq. (11), we have further calculated the temperature for which the viscosity reaches the value of $\eta_s = 10^{11}$ Pa s. These temperatures are also given in Table I in the last column. They are in good agreement with the glass transition temperatures determined by DSC. Thus from our data we have no evidence for assuming an Arrhenius type of activated process in the vicinity of T_g which has been observed sometimes for other systems.[31] From the data it is evident that OTP and BCDE behave dynamically similar as their activation parameters are in a comparable range. This finding is further supported by Hagenah,[32] who has measured the dynamics of the α relaxation (which corresponds to density fluctuations of BCDE) by photon correlation spectroscopy in the vicinity

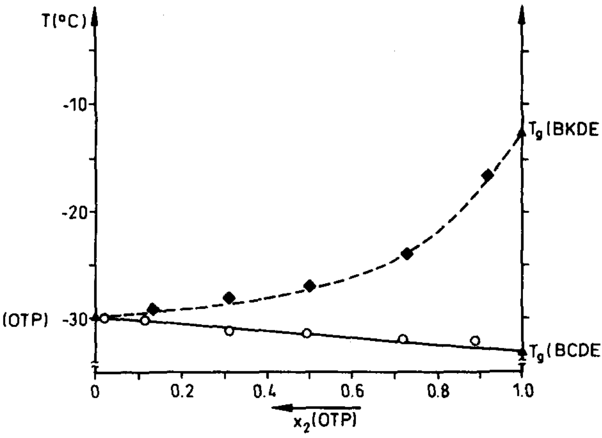

FIG. 1. Glass transition temperatures of mixtures of BCDE/ OTP (○) and BKDE/ OTP (◆) plotted vs the mole fraction x_2 of OTP.

TABLE I. Fit parameters of the VFT equation [Eq. (11)] from viscosity measurements. T_g has been measured by DSC, T_g' is calculated from the VFT equation with $\eta = 10^{11}$ Pa s.

	$\log \eta_0$	B (K)	T_∞ (K)	T_g (K)	$T_g'(\eta = 10^{11}$ Pa s) (K)
BKDE	-8.6 ± 1.0	2660 ± 300	205.7 ± 3.5	260.8	264.6
BCDE	-8.2 ± 0.8	2122 ± 299	191.1 ± 5.7	240.1	239.1
OTP	-8.2 ± 3.8	1936 ± 480	199.4 ± 6.0	243.5	243.2
BCDE/OTP ($x_1 = 0.31$)	-10.6 ± 1.4	2845 ± 582	182.0 ± 7.7	241.9	239.6
BKDE/OTP ($x_1 = 0.50$)	-8.4 ± 0.4	2359 ± 196	190.1 ± 3.8	246.2	243.0

of T_g and has found $B = 1797 \pm 55$ K and $T_\infty = 200 \pm 10$ K. The B and T_∞ values for OTP reported here are in good agreement with those from the literature.[33]

C. Measurements of n_D

We have further measured the index of refraction n_D^{20} of the materials by means of an Abbe refractometer in a temperature range from 45 to 90 °C. The values at $T = 20$ °C were obtained by linear extrapolation. For OTP we found $n_D^T = (1.6421\text{–}4.5)\times 10^{-4}\Delta T(°\mathrm{C})$ (cf. Ref. 34); for BKDE, $n_D^T = (1.5707\text{–}3.5)\times 10^{-4}\Delta T(°\mathrm{C})$; and for BCDE, $n_D^T = (1.5847\text{–}3.4)\times 10^{-4}\Delta T(°\mathrm{C})$. For the mixtures we performed the same experiment, thus giving $(\partial n/\partial x_i)^2$ for the two mixtures of 0.0034 for BKDE/OTP and 0.0033 for BCDE/OTP. For $T = 42$ °C the densities of these pure materials were measured with a pyknometer calibrated with toluene within 0.1% to literature values to give for OTP, $\rho^{28,5} = 1.059$ g/cm^3 (cf. also Ref. 34); for BKDE, $\rho^{27} = 1.070$ g/cm^3; for BCDE, $\rho^{27} = 1.065$ g/cm^3.

D. Sample preparation and light-scattering experiment

Pure materials and all mixtures were prepared to yield suitable samples for the purpose of light scattering by filtration through a 0.22 μm Millipore Teflon filter directly into a dust-free light-scattering cell with 1/2 in. o.d. using a hot syringe. After that, the samples were flame sealed under vacuum.

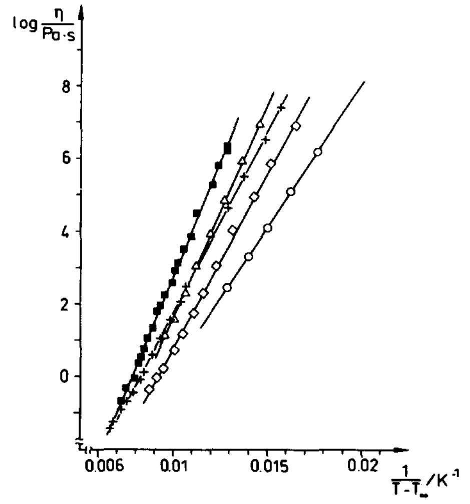

FIG. 2. Logarithm of the steady-flow viscosity vs $(T - T_\infty)^{-1}$ for BKDE (■), BCDE (◇), OTP (○), BCDE/OTP with $x_1 = 0.31$ (△), BKDE/OTP with $x_1 = 0.5$ (+)

The light-scattering experiment was performed at different temperatures either at a fixed scattering angle of $\theta = 90°$ or at various angles in the range of 40° up to 130° in a home-built goniometer to check the angular dependence of the dynamics. The goniometer was calibrated with toluene to give an angularly independent intensity within ± 5% after correction for the scattering volume. The light source was an argon ion laser (Spectra Physics model 2020) operating at $\lambda = 488$ nm with a power of 400 mW. The incident and the scattered laser beam were polarized perpendicular to the scattering plane, so that the geometry of the measurement was the so-called *VV* geometry. The full correlation functions were obtained using a 128-channel Brookhaven correlator (BI2030) in the multiple τ version. To provide a greater time range of up to seven decades usually two runs with different basic sample times were spliced together using a procedure described elsewhere.[35]

E. Data analysis

The desired normalized correlation function $(\mathbf{q},t)$ of the scattered electric field is related to the measured intensity time correlation function $G(\mathbf{q},t)$ through the Siegert relation:[1]

$$G(\mathbf{q},t) = \langle I_q(0) I_q(t)\rangle = A(1 + f\alpha^2 |g(\mathbf{q},t)|^2). \tag{12}$$

There A is the base line which can be computed in the course of experiment by $A = N\cdot\langle n\rangle^2$ with N being the total number of duty cycles and $\langle n\rangle$ being the mean number of photon counts per delay times $\Delta\tau$; t is given by $t = I\cdot\Delta\tau$ where I is the number of channels. The base line can also be measured by delayed channels of the correlator. In our cases the differences between the calculated and measured base lines were always less than 0.5%, indicating that no further slow processes will be hidden in the long-time tail of the measured correlation function. The factor f depends mainly on the size and distance of pinholes determining spatial coherence. The factor α is the fraction of the total intensity $\langle n\rangle$ which relaxes within the time window of the correlator.[35] Although it is known that concentration fluctuations show a Debye relaxation behavior, we use the widely accepted Kohlrausch–Williams–Watts (KWW) function to account for the time decay of $g(\mathbf{q},t)$ via

$$g(\mathbf{q},t) = \exp\left\{-\left[\frac{t}{\tau_{\mathrm{KWW}}(\mathbf{q})}\right]^\beta\right\} \tag{13}$$

with $0 < \beta \leqslant 1$ being a measure of the width of the distribution. α, τ_{KWW}, and β are treated as fit parameters in Eqs. (12) and (13). For density fluctuations up to now no $\mathbf{q}$ dependence has been observed,[35] β is considerably lower than one[36] and a mean relaxation time $\langle\tau\rangle$ can then be calculated by

$$\langle\tau\rangle = \frac{\tau_{KWW}}{\beta}\Gamma(\beta^{-1}) \quad (14)$$

with Γ being the gamma function. For concentration fluctuations β are almost equal to one and the decay time $\tau_{KWW}(\mathbf{q})$ ($\cong \tau_c$) from Eq. (13) is related to the mutual diffusion coefficient D by

$$\tau_c = (Dq^2)^{-1} \quad (15)$$

with q being $|\mathbf{q}|$. Thus a translational diffusion process will scale with q^{-2}, whereas density fluctuations do not.

Since the measured correlation functions show at least two distinct processes within the accessible time window of the experiment, we have used up to two KWW functions to account for the proper mathematical description of the correlation functions. As Eq. (13) only shows the general route of describing data, we have not reproduced the formula for a double KWW function but refer to the literature[37] instead. We have found that, in general, the processes are well separated such that no disturbing interference between the individual processes occurs. Thus, we have not used the method of inverse Laplace transformation to obtain the distribution of relaxation times,[38] but we think that a KWW analysis is sufficient to represent the data.

IV. RESULTS AND DISCUSSION

We have measured the mixtures BKDE/OTP with $x_1 = 0, 13, 0.31, 0.5$ and BCDE/OTP with $x_1 = 0.11, 0.31, 0.49$ with the maximum temperature range from 0 °C to 100 °C. In Fig. 3 we show the experimental net correlation functions $|\alpha g(t)|^2$ for BKDE/OTP with $x_1 = 0.33$ at different temperatures; in Fig. 4 those for BKDE/OTP with $x_2 = 0.5$; in Fig. 5 those for the mixture BCDE/OTP with $x_1 = 0.49$. In general, the composite correlation functions show a complicated time behavior which is governed at the most by three processes which, however, cannot be measured all together within the accessible eight decades in time. At the lowest measured temperature of 0.6 °C we observe in Fig. 3 a process at the short-time end with low contrast and obviously broad distribution of relaxation times followed by a strong, almost single-exponential decay at about 1 s. By raising the temperature both processes are accelerated so that the first process is shifted out of the time window of our correlator. At the long-time end another process which is also almost single exponential in shape appears. At 40 °C the last two processes are conveniently within the time window. In principle, the same description holds for Fig. 4, where especially for $T = 61.1$ °C the separation between both processes can be clearly observed. The same features also hold for the mixture BCDE/OTP as can be seen in Fig. 5.

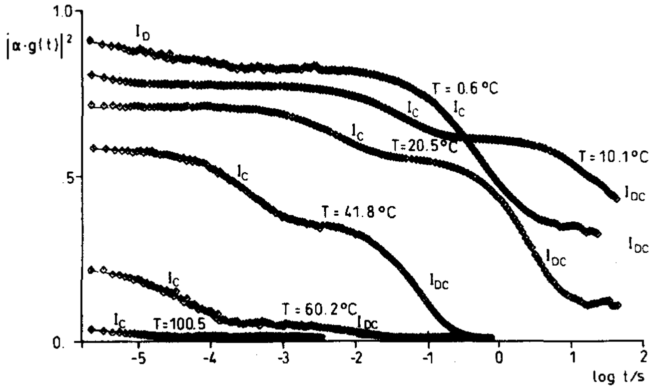

FIG. 3. Correlation function $|\alpha g(t)|^2$ for the BKDE/OTP mixture with $x_1 = 0.31$ at various temperatures indicated. I_D denotes the density fluctuation, I_C denotes the interdiffusion process, and I_{DC} refers to the cluster diffusion.

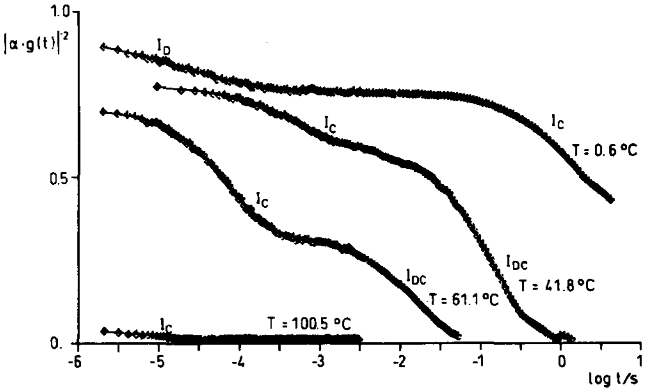

FIG. 4. Correlation function $|\alpha g(t)|^2$ for the BKDE/OTP mixture with $x_1 = 0.5$ at various temperatures as indicated. For further assignment see Fig. 3.

On the basis of these results we postulate that the dynamic behavior of the mixtures can be described by the superposition of three independent processes:

$$I_{\text{total}} = I_D + I_C + I_{DC}, \quad (16)$$

with relaxation times

$$\tau_D \ll \tau_C \ll \tau_{DC}, \quad (17)$$

and with relaxation strengths

$$\alpha_D \ll \alpha_C + \alpha_{DC}. \quad (18)$$

The indices refer to the origin of the relaxation processes. As

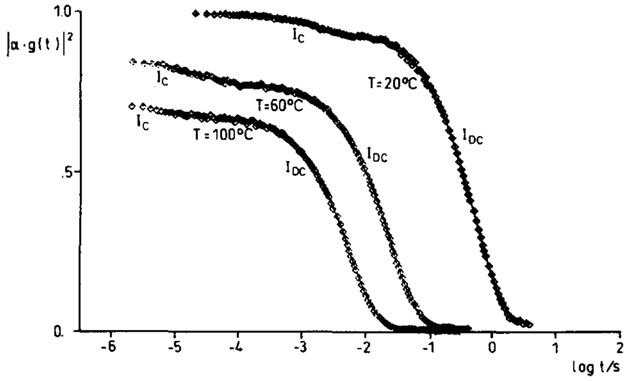

FIG. 5. Correlation functions $|\alpha g(t)|^2$ for the BCDE/ OTP mixture with $x_1 = 0.49$ at various temperatures as indicated. For further assignment see Fig. 3.

we will show in the following, I_D is due to density fluctuations, I_C is caused by concentration fluctuations, and I_{DC} by an unknown process, which we will identify preliminarily as "cluster diffusion." Since the time scale of the processes is very different, the evaluation can be performed on the basis of Eqs. (5) and (13).

The results of the KWW evaluation are listed in Tables II and III. The average relaxation times have been calculated from Eq. (14).

In order to clarify the origin of the various processes three additional experiments were carried out: (i) scattering in the *VH* geometry, (ii) measurements of the q dependence of the relaxation times, and (iii) investigation of the effects of thermal history. Additionally, the results of static q-dependent light scattering $I_{\rm tot}(q)$ are taken into account.

For the pure substances OTP and BCDE,[32] we observe the density fluctuation in the *VH* geometry almost with the same relaxation times as measured in *VV*, which may be due to a strong dynamic coupling between fluctuations of density and anisotropy. Thus we conclude from this experiment that the fluctuation of density is responsible for the fast process of low contrast with a broad distribution of retardation times showing up in Fig. 4 at a temperature of 0.6 °C. The broad distribution is a result of the KWW fit [Eq. (13)] to the correlation function giving β parameters of about 0.5, as listed in Table IV. We notice that I_D is observable only at a few low temperatures, and further that β_D is rather small in all cases and that $-\log\langle\tau\rangle_D$ for comparable temperatures does not depend appreciably on concentration. β parameters considerably deviating from 1 (the typical value for concentration fluctuations [see Eq. (15)], are usually found for density fluctuations both in polymeric systems[35,36] and nonpolymeric glassy liquids.[34,38] If we use the T_∞ values from the fit of Eq. (11) to the shear viscosity η_s data we can construct a masterplot for the density fluctuations for all pure and mixed materials as seen in Fig. 6. This result clearly resembles the fact of the applicability of the time–temperature superposition principle to the density fluctuations as revealed by Eq. (6), relating mechanical properties with the time autocorrelation function of density fluctuations.

The reason for the different relaxation strengths α for I_D and $I_C + I_{DC}$ simply arises from the fact that $(\partial\epsilon/\partial\rho)^2\langle\delta\rho^2\rangle$, being responsible for the amplitude of the density fluctuations, is generally smaller than $(\partial n/\partial x)^2\langle\delta x^2\rangle$ (being responsible for the amplitude of concentration fluctuations) provided that both components are not index matched. (For our systems that is not the case.) Thus most of the scattered intensity arising from our mixtures is due to the second and third terms in Eq. (5).

Now we turn to the process which we have assigned with I_C. It is evidently a property of the mixture because this process cannot be seen in pure OTP.[39] In the theoretical section we have given by Eq. (10) an expression for the intensity due to concentration fluctuations in a binary mixture. We have calculated $I_C^{\rm id}$ by using $(\partial n/\partial x_i)$ values as given in the experimental part. Assuming ideal mixture behavior, we have used the measured densities of the pure components to calculate $V_{\rm mix}$. The results are shown in Fig. 7. From the calculation it follows that the mixture BCDE/OTP behaves ideally, whereas the system BKDE/OTP exhibits an enthalpic scattering and thus deviates considerably from ideality. The difference between $I_C^{\rm id}$ and I_C for BCDE/OPT is actually within the experimental error. The amplitude of I_C for that system varies from 0.008 for $x_1 = 0.02$ up to 0.03 for $x_1 = 0.49$, thus the experimental determination of R_{vv}^{c} is uncertain. This emphasizes the weak scattering from an ideal solution. For the BKDE/OTP system the corresponding values range from 0.03 up to 0.11. We were further interested in a rough calculation of the interaction parameter χ in the BKDE/OTP system. For that purpose we have calculated $I_C^{\rm id}/I_C$ for this mixture, which is related to thermodynamic quantities via[8]

$$\left[1-\frac{I_C^{\rm id}}{I_C}\right]=\frac{x_1x_2}{RT}\left[\frac{\partial^2G^{\rm excess}}{\partial x_1\,\partial x_2}\right]. \tag{19}$$

Examples of such calculations have been performed for mixtures of simple organic liquids.[7,8] There qualitatively similar

TABLE II. Logarithm of the mean relaxation times [Eq. (14)] and β-distribution parameters of the diffusive processes for BKDE/OTP mixtures. The suffix *C* denotes interdiffusion and *DC* denotes cluster diffusion.

	Mole fraction x_1	T(°C)	$-\log\langle\tau\rangle_C$	β_C	$-\log\langle\tau\rangle_{\rm DC}$	β_{DC}
BKDE/OTP	0.13	10.1	0.72	0.94	···	···
		20.2	2.33	1.00	−1.11	0.89
		30.0	3.12	1.00	−0.26	0.91
		40.0	3.70	0.87	0.48	0.86
	0.31	0.6	−0.26	0.76	< −3.5	···
		10.1	0.92	0.85	∼ −2.0	···
		20.5	2.18	0.92	−0.76	0.98
		40.0	3.47	0.93	0.82	0.97
		60.2	4.22	0.85	1.72	0.96
		100.5	4.85	1.00	···	···
	0.50	0.6	∼0.57	0.85	···	···
		41.8	3.14	0.96	0.47	0.92
		61.1	4.03	0.93	1.44	0.92
		100.5	4.85	1.00	···	···

TABLE III. Logarithm of the mean relaxation times [Eq. (14)] and β-distribution parameters of the diffusive processes for BCDE/OTP mixtures. The suffix C denotes interdiffusion and DC denotes cluster diffusion.

	Mole fraction x_1	T (°C)	$-\log\langle\tau\rangle_C$	β_C	$-\log\langle\tau\rangle_{DC}$	β_{DC}
BCDE/OTP	0.112	10.1	2.13	0.79	− 1.18	0.85
		30.0	3.80	0.83	0.64	1.00
		40.1	3.85	0.92	0.96	0.90
		60.3	4.77	0.81	1.70	1.00
		80.0	···	···	1.92	0.89
	0.310	10.1	1.64	0.96	− 1.08	1.00
		40.2	3.80	1.00	1.17	0.99
	0.494	20.1	2.92	1.00	− 0.04	0.97
		60.1	4.66	0.93	1.30	0.94
		100.5	···	···	1.92	0.94

behavior was found. The excess free energy G^{excess} is related to the ΔG of mixing simply by adding TS^c, where S^c is the configuration entropy given by

$$S^c(x) = -R(x_1 \ln x_1 + x_2 \ln x_2). \tag{20}$$

The free energy of mixing ΔG is given by

$$\Delta G = RT[x_1 \ln x_1 + x_2 \ln x_2 - \chi x_1 x_2], \tag{21}$$

where χ is the interaction parameter accounting for enthalpic interaction. Hence the use of Eq. (19) together with Eq. (21) gives an estimate of the magnitude of χ for our BKDE/OTP system to be about -2.6 at $T = 40\,^\circ\mathrm{C}$. We note here that the deviation from the linear dependence of the glass transition temperatures as a function of the volume fraction (see Fig. 1) is probably connected to the deviations from the ideal solution properties. Such a relationship between the nonideal behavior and enthalpic interactions has been speculated in the literature recently.[40]

In polymeric systems the interaction is strongly enhanced by the long molecular chains which are characterized by the degree of polymerization (N). This interaction usually leads to demixing phenomena or phase separation. Here in the case of the mixture of van der Waals liquids, the ΔG is mostly governed by entropic effects. Besides the static (thermodynamic) properties we have further investigated the dynamic aspects of I_C (and subsequently I_{DC}). Especially, as already introduced to be our second point, we have measured the q dependence of the dynamics, since we expect

TABLE IV. Logarithm of the mean relaxation times [Eq. (14)] and β-distribution parameters for the density fluctuations in pure materials and mixtures. The suffix D denotes density fluctuations.

	Mole fraction x_1	T (°C)	$-\log\langle\tau\rangle_D$	β_D
BKDE		− 15.3	− 1.85	0.39
		− 10.2	− 0.93	0.43
		− 5.4	0.51	0.54
		− 0.3	1.02	0.45
		− 0.2(VH)	1.22	0.46
		5.3	2.08	0.55
		10.2	2.52	0.45
		15.3	3.15	0.38
		20.2	4.80	0.27
BCDE		− 18.6	0.66	0.56
		− 9.7	2.37	0.52
		− 5.2	4.00	0.49
BKDE/OTP	0.500	− 18.6	0.35	0.52
		− 10.2	1.39	0.39
		− 5.3	2.39	0.55
		− 5.3(VH)	2.46	0.57
		0.6	3.60	0.48
	0.31	− 9.9	2.42	0.50
		0.6	4.89	0.47
		10.1	5.60	0.60
BCDE/OTP	0.02	− 10.2	2.23	0.53
	0.13	− 9.7	2.70	0.56
	0.49	− 10.2	2.74	0.50
	0.3	10.0	4.72	0.62

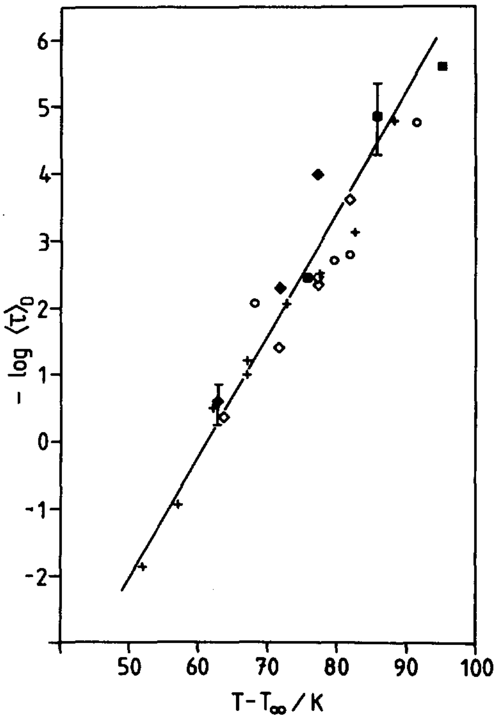

FIG. 6. Master curve construction of τ_D, the correlation time of the density fluctuation, measured in all mixtures (◇, BKDE/OTP with $x_1 = 0.5$; ■, BKDE/OTP with $x_1 = 0.31$; ○, BCDE/OTP with $x_1 = 0.13, 0.33, 0.49$) and pure liquids (+ , BKDE; ◆, BCDE) and scaled with the fitparameter T_∞ of viscosity measurements from Eq. (11).

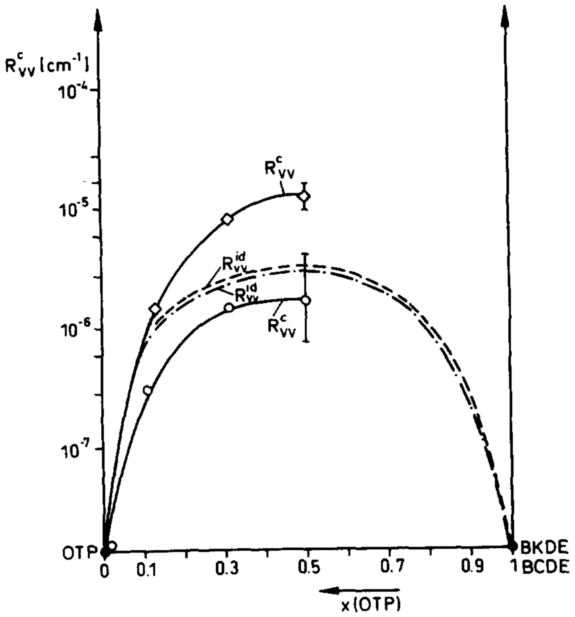

FIG. 7. The experimentally determined Rayleigh ratios R^c_{vv} for the interdiffusion mode I_C for BKDE/OTP (◇) and BCDE/OTP (○) in comparison with the ideal contribution R^{id}_{vv} for BKDE/OTP (---) and BCDE/OTP (-·-) according to Eq. (10). Error in the estimation of $[\partial n/\partial x]$ for $R^{id}_{vv} \simeq 10\%$.

a q^{-2} scaling according to Eq. (15) when dealing with translational diffusion processes. In Fig. 8 typical results at various scattering angles for the mixture BKDE/OTP with $x_1 = 0.31$ are shown. We note a clear shift of both obvious diffusional processes with lowering q towards longer times which is in accordance with the theoretical prediction. The plots of $\langle\tau\rangle^{-1}$ vs q^2 shown in the right in Fig. 8 give straight lines through the center in both cases. From the slope, D can be calculated (cf. Fig. 8 caption). The density fluctuations are not to be seen as they are too fast already; compare also with the correlation function at the same temperature ($T = 40$ °C) in Fig. 4.

From the inspection of the correlation function in Fig. 8 we conclude that the relaxation strength of the slow process obviously depends on the scattering angle θ. We have to consider, however, the effect of change of the total intensity with θ. If the relaxation, which corresponds to a dynamic process, will fall into the time window of our experiment having the intensity I_{relax} we simply relate $I_{\text{total}} = I_{\text{density}} + \sum I_{\text{concentration}}$ with the relaxed intensity of our process[3] under study by $I_{\text{relax}} = \alpha \cdot I_{\text{total}}$. We have found that the I_{total} exhibits an angular dependence which correlates well with the intensity of the slow diffusion process given by $I_{DC} = \alpha_{DC} I_{\text{total}}$. On the other hand, the intensity I_C, which corresponds with the fast diffusive process, $I_C = \alpha_C I_{\text{total}}$, does not change with θ.

In Fig. 9 we show the dependence of the intensity of the fast and slow concentration fluctuations as a function of q for the same mixture and the same temperature as given in Fig. 8. We have measured the scattered intensity down to a scattering angle of $\theta = 40°$. The data points from the quasielastic scattering (cf. Fig. 8) are also implemented. The intensities are corrected for the change of scattering volume with θ. Clearly the intensity of the fast process does not exhibit any angular dependence and is shown as a solid line parallel to the x axis in Fig. 9, whereas the slow one does, in accordance with the findings derived from Fig. 8 that the intensity of the slow process increases with decreasing θ due to strong forward scattering. The described feature is common for all the mixtures where an additional slow process shows up. The two systems under study, BKDE/OTP and BCDE/OTP, differ with respect to the occurrence of this phenomenon in a way that the latter system shows this slow mode at all measured temperatures without actually changing its intensity, whereas for the former mixture we observe a breakdown of the slow mode at about 60 °C. This explains the completely different shapes of the correlation functions in Figs. 4 and 5 for temperatures higher than 60 °C. We will not comment further on this experimental finding at this stage, but concentrate on the physical nature of the two diffusional processes. We take Figs. 8 and 9 as proof of the fact that large extended structures which diffuse slowly are responsible for the slow mode ("cluster diffusion"). Then consequently the fast diffusional mode is the interdiffusion mode we would have actually expected to appear in our mixtures based on

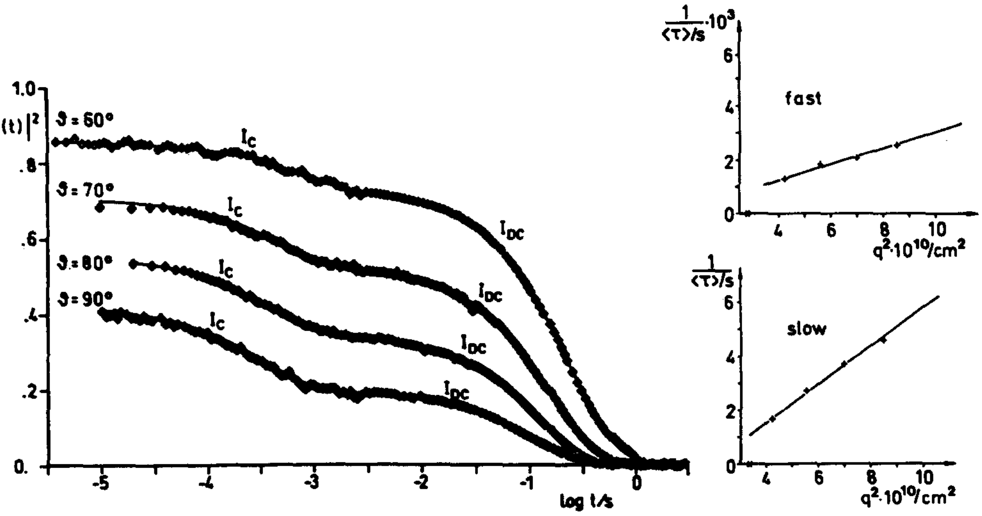

FIG. 8. On the left: Correlation functions for the BKDE/OTP mixture with $x_1 = 0.31$ for $T = 41.8$ °C at various scattering angles as indicated. On the right: $\langle\tau\rangle^{-1}$ vs q^2 for the two diffusional processes. Upper curve for the interdiffusion mode giving $D = 2.95 \times 10^{-8}$ cm^2 s^{-1}; lower curve for the cluster diffusion $D = 5.38 \times 10^{-11}$ cm^2 s^{-1}. For the assignment of the process see Fig. 4.

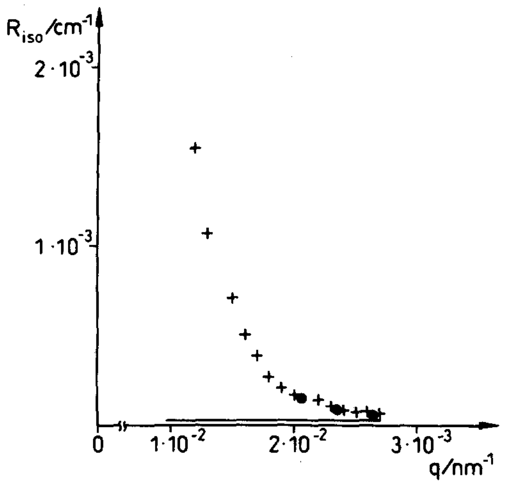

FIG. 9. The scattered intensity vs the scattering vector for the mixture BKDE/OTP with $x_1 = 0.31$ at $T = 41.8$ °C from totally scattered intensity measurements (+) and from PCS (●). The solid line at the bottom denotes the background according to interdiffusion and density fluctuations.

the theoretical treatment of light scattering.[1]

At this stage we have accounted for the nature of the different modes showing up in Figs. 3–5. Analyzing the correlation function in terms of stretched exponentials as outlined by Eq. (13), we calculate mean relaxation times by Eq. (14) for each individual relaxation mode and plot the results as Arrhenius plots in Figs. 10 and 11 for BKDE/OTP with $x_1 = 0.31$ and $x_1 = 0.5$ and in Fig. 12 for BCDE/OTP with $x_1 = 0.11, 0.31, 0.49$. In all plots we have made use of the possibility of a master curve construction for the density fluctuation. To do so we have used photon correlation spectroscopy (PCS) data for pure OTP,[32,34] and further assume that in the mixtures the dynamics of I_D is only governed by the temperature distance to T_g(mix). For each figure it is evident that there are almost parallel lines for I_C and the slowest relaxation mode, and further the different activation

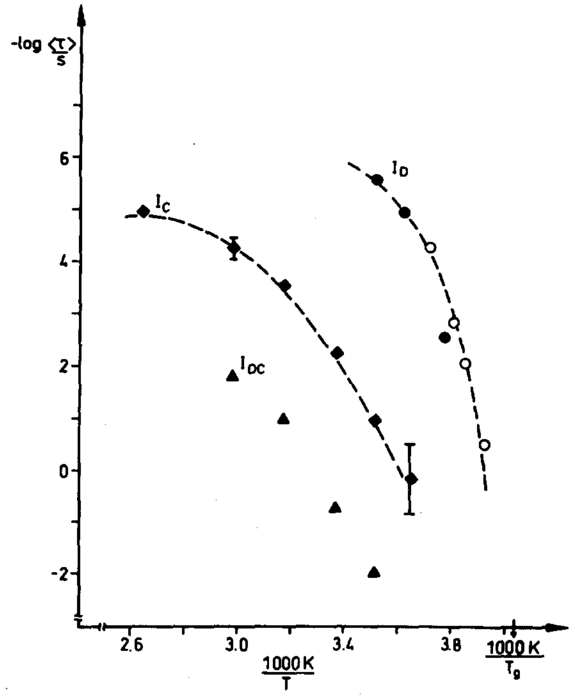

FIG. 10. Arrhenius plot for the mixture of BKDE/OTP with $x_1 = 0.31$ with a master curve construction for the density fluctuation whereby we use open symbols for shifted values and solid symbols for those measured in the mixtures. The lines are the results of a fit of the Vogel–Fulcher–Tammann equation [Eq. (11)] to the data.

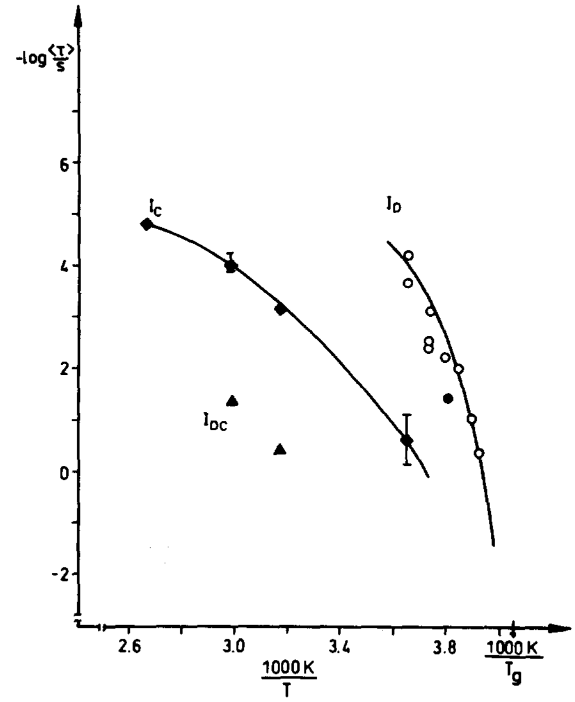

FIG. 11. Arrhenius plot for the mixture of BKDE/OTP with $x_1 = 0.5$; otherwise, see caption of Fig. 10.

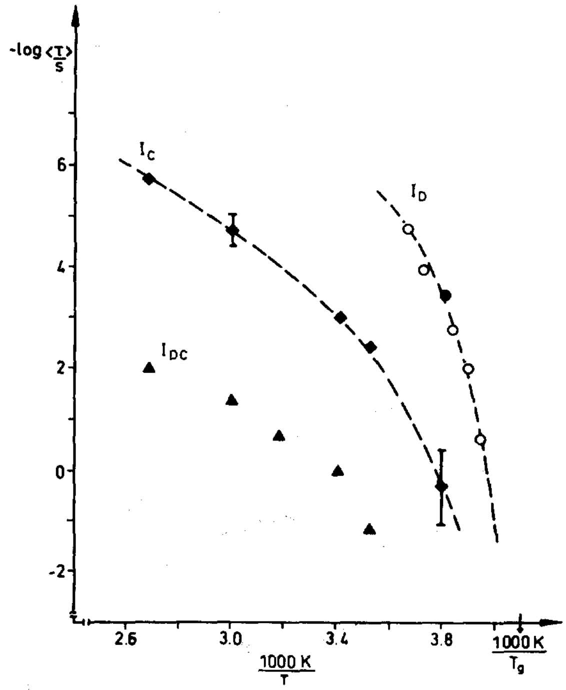

FIG. 12. Arrhenius plot for the mixture of BCDE/OTP with $x_1 = 0.49$; otherwise, see caption of Fig. 10.

energies for I_C and I_D obviously lead to a merging at low temperatures. Unfortunately, we were not able to directly measure this effect because the expected relaxation times for this will lie roughly in the range of minutes and longer, and thus are not accessible for PCS. Different activation energies for the density fluctuation and concentration fluctuation modes are also reported by Floudas, Fytas, and Ngai[14] for the system poly(cyclohexylmethacrylate) in mixtures with dioctylphtalate (DOP), a commonly used plasticizer, and previously in poly(methylphenylsiloxane) contaminated with oligomers.[12] There the argument is based on the coupling model by Ngai,[41] which claims that the activation barrier for the primitive microscopic relaxation is related to the cooperative activation energy B from the VFT equation [Eq. (11)], β is related to the distribution parameter from the KWW representation [Eq. (13)], which basically is a result of the assumption of a time-dependent primitive relaxation rate, thus accounting for a slowing down of the dynamics when approaching T_g. The model simply yields

$$\frac{B_0}{\beta} = B_{\text{cooperative}}, \tag{22}$$

where B_0 is the primitive activation barrier. B_0 as given by Eq. (1) is usually discussed to be a monitor of the temperature dependence of the local friction ξ_0 by

$$\xi_0 \propto \exp\left(\frac{B_0}{T - T_0}\right). \tag{23}$$

Thus its relation to the measured diffusion constants is provided by

$$D = \frac{kT}{\xi_0} \tag{24}$$

in the absence of a structure factor.

If we identify the concentration fluctuation I_C with the primitive relaxation because of its direct correlation to the friction [Eq. (24)] which governs the mass transport, then according to Eq. (22) we should observe for the B_0 parameter following Eq. (23) a value of $0.43 \times 2359 = 1014$ K for BKDE/OTP with $x_1 = 0.5$. The β value for I_D is taken from Table IV. Usually β values for density fluctuations of molecules of this kind are higher.[34] If we take a reported value of 0.55 we get $B = 1297$ K. We have fitted Eq. (23) to the I_C data given in Fig. 11 and found $B = 1357$ K with $T_\infty = 197$ K in close agreement with the T_∞ given in Table I. Due to the difficulties in determining the range of I_D for the other systems, we did not compare our results any further, but state that in the one example the agreement with Eq. (22) is good.

Now we turn to the slowest process which shows up in all correlation functions of BCDE/OTP, and for BKDE/OTP only for temperatures below 60 °C. We have already stated that this mode is due to the motion of huge species or spatially extended domains—we have called them clusters—causing an angular dependence of the scattered intensity as depicted in Fig. 9. Using for convenience the data BKDE/OTP with $x_1 = 0.3$, we have calculated the translational diffusion coefficient at $T = 41.8$ °C from Eq. (6) to give $D = 5.4 \times 10^{-11}$ cm^2/s. Introducing the measured viscosity from Fig. 2 into Stoke's law, we have estimated an apparent diameter for the diffusing cluster of 210 nm in the rigid noninteracting spheres approximation. On the other hand, we assume a simple pair correlation function of the form

$$f(r) \propto \exp(r/\xi), \tag{25}$$

where ξ is a measure of the spatial extension of inhomogeneities (here cluster boundaries) in our sample. For a correlation function given by Eq. (25) it can be shown that the intensity caused by scattering from such an assembly is given by[42]

$$I_{\text{ex}} \propto \frac{\langle \Delta\epsilon \rangle^2 \xi^3}{(1 + q^2\xi^2)^2}. \tag{26}$$

Thus from our $I_{\text{ex}}(q)$ data we can estimate ξ by plotting $1/\sqrt{I}$ vs q^2 to give a straight line as depicted in Fig. 13. Other correlation functions have not given reasonable results.[43] From Fig. 13 we have calculated $\xi = 215 \pm 20$ nm from the slope and positive intercept. Figure 13 may suggest a negative intercept which is physically unreasonable. However, the points around $q^2 = 4 \times 10^{-1}$ nm^2 are those with the highest precision. Extrapolation from those led to the given line. Furthermore, we have undertaken measurements on pure OTP in a larger scattering cell to improve the precision at lower angles[44] and found agreement with the extrapolation given in Fig. 13 having a positive intercept. Especially if one follows Debye's paper, the $\Delta n = \Delta\epsilon/2n$, where $\Delta\epsilon$ is from the fit, can be estimated to be to 3.3×10^{-4} in good agreement with the reported value for poly (methylmethacrylate), PMMA.[24] The calculated value of ξ can be compared with the apparent diameter from Stoke's law using the dynamic results. Both values are in good agreement, indicating that they are complementary to each other in the sense that if we find cluster diffusion of species larger than 100.0 nm, we observe an angularly dependent intensity. In pure OTP we observe cluster diffusion above T_m exhibiting a dif-

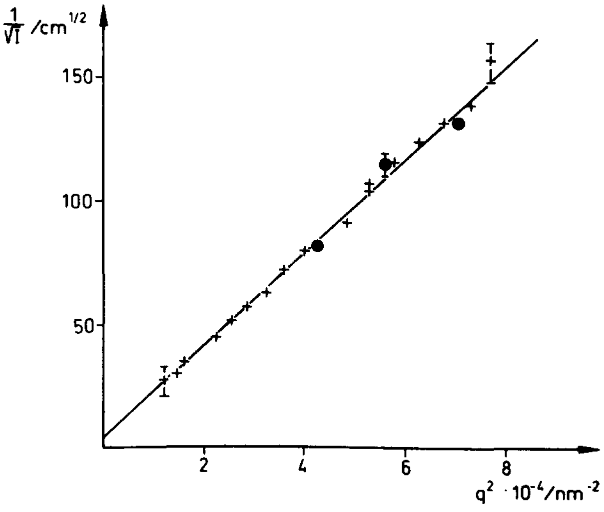

FIG. 13. $I^{-1/2}$ vs the square of the scattering vector for BKDE/OTP with $x_1 = 0.3$ at $T = 41.8$ °C (+, totally scattered intensity); ●, (PCS). The intensity is corrected by subtraction of the background (cf. Fig 7). From the slope and intercept we have determined the correlation length to be $\xi = 215 \pm 20$ nm (see Ref. 43).

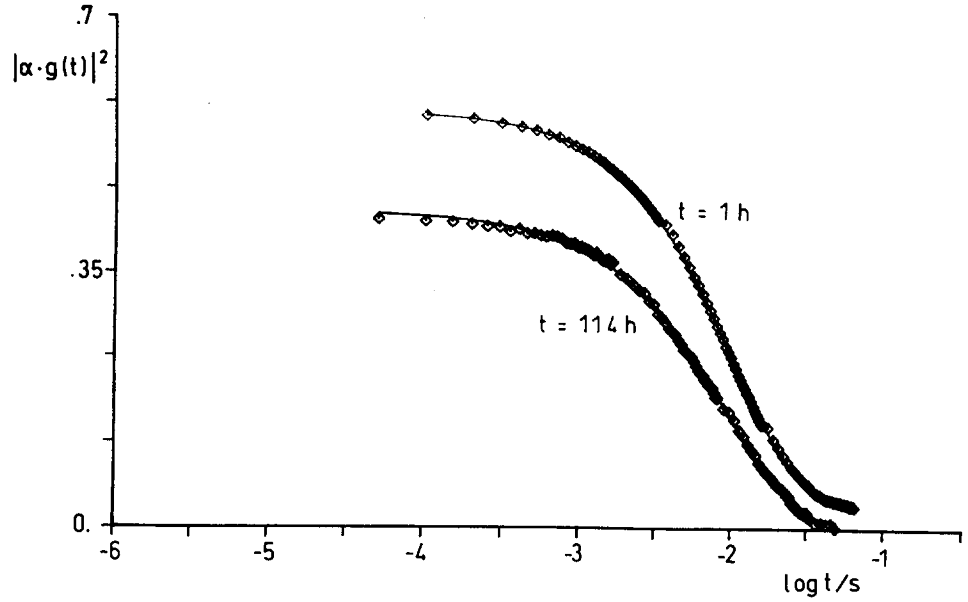

FIG. 14. Correlation function for the mixture of BCDE/OTP with $x_1 = 0.49$ after 1 h of temperature exposure at $T = 93.3$ °C (upper curve) and after 114 h exposure (lower curve).

fusion constant also roughly three orders of magnitude smaller than the self-diffusion.[44] Furthermore, we were able to show to what extent this phenomenon accounts for the excess scattering into the central line of a polarized Rayleigh–Brillouin experiment. The cluster diffusivity causes a nonzero $[\partial n/\partial x]$. Otherwise, it would not contribute to a dynamic light-scattering experiment. Consequently, the scattering into the central line is enhanced, leading to high values of I_{central},[21] thus increasing the Landau–Placzek ratio which deviates considerably from the prediction of the theory.[45] The appearance of clusters in liquids has already been treated thoroughly in the Introduction. The purpose of this argument is simply to relate our observations to those reported there to put everything into a common framework. The cluster concept is not new. It was introduced by Frenkel[46] and Ubbelohde[47] a long time ago. Now the experimental evidence has become so substantial (cf. references given in the Introduction) that obviously the effect cannot be neglected as was done in the past by saying it is dust, dirt, or anything else. However, a lot of questions arise when dealing with this phenomenon. What is the thermodynamically stable state? How are clusters created and destroyed? And, are there any kinetic effects involved? Not all these questions can be solved, however, when analyzing our mixtures. The striking difference in the BKDE/OTP and BCDE/OTP systems in terms of cluster formation can speculatively be related to ideas outlined by Frenkel,[46] who treated thermodynamically pretransitional ordering in a system containing embryos of species A in a matrix of B having a phase boundary. In his formula the surface energy enters which is empirically connected with the enthalpic interaction of the system. Thus we assume a more drastic temperature effect for the BKDE/OTP system than for BCDE/OTP, which is indeed correct. For the more interacting system we find a decrease of the apparent diameter with rising temperature finally reaching a point where no clusters are further detectable (cf. Figs 3 and 4). Since the effects are generally more pronounced in mixed systems, we speculatively assume that the interaction between different molecules acts as a magnifier to monitor the cluster formation which is generally present in any pure liquid,[48] as in pure OTP.

We have further investigated kinetic experiments because we were interested to know something about time effects. For this purpose we chose the BCDE/OTP with $x_1 = 0.5$ system and heated the mixture for 114 h at a temperature of 92 °C. In Fig. 14 the correlation functions for the slow mode are shown, indicating a decrease in relaxation strength with a constant decay time otherwise, indicating a decrease of the number of diffusing particles not of their size. This dynamic finding is also in agreement with measurements of the intensity, where we found no change in ξ with the time of exposure.

Hence we can reach a stage where no clusters are present if the temperature is high enough and the time of exposure at that temperature long enough. By deep quenching such a state to a temperature where usually we observe clusters, the cluster free state can be kept stable for some time. However, slowly cluster formation occurs. In detail that effect depends on the rate of quench, the temperature difference to T_g, and the kind and magnitude of interactions in the system.

At this state it is too early to draw a complete construction of our understanding of cluster formation, but following the idea outlined in the Introduction, we come to the starting point again. We feel that the cluster formation and its experimental manifestation has gained further support.

ACKNOWLEDGMENTS

G. M. gratefully acknowledges the financial support from the Sonderforschungsbereich–262. The authors are indebted to Professor A. Patkowski for carefully reading the manuscript and for valuable comments, and also to Professor G. Fytas for reading the manuscript.

APPENDIX: CHEMICAL SYNTHESIS

Synthesis of the two low molecular weight liquids 1,1-di(paramethoxyphenyl)-cyclohexane (a) (BCDE) and 1,1-di(paramethoxy-metamethylphenyl)-cyclohexane (b) (BKDE) used for all the discussed measurements:

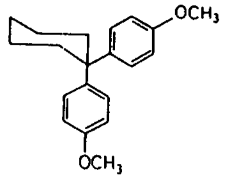

(a)

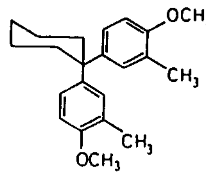

(b)

1. Synthesis of compound (a) BCDE

According to a previously published procedure[49,50] cyclohexanone was condensed under acidic conditions with phenol to give a product in a yield of 87% after purification; mp 187 °C (literature mp 186 °C).

In a standard procedure the 1,1-di(parahadroxyphenyl)-cyclohexane was treated with an excess of 2–3 mol of dimethylsulfate dissolved in 10% aqueous solution of NaOH. Purification of the crude product was done using a middle pressure liquid chromatography (MPLC) system with CH_2Cl_2 as eluent and subsequent recrystallization from methanol to give the product with a purity of 99.8% according to high pressure liquid chromatography (HPLC) analysis; mp 58 °C.

Elementary analysis: $C_{18}H_{20}O_2$, $M = 296.39$ g/mol.

Calc.: C, 81.04; H, 8.16.

Found: C, 81.25; H, 8.26.

^{1}H–NMR (CD_2Cl_2): $\delta = 1.54$ (*m*, cyclohexyl), $\delta = 2.24$ (*m*, cyclohexyl), $\delta = 3.76$ (*s*, O–CH_3), $\delta = 6.82$ (*d*, phenyl), $\delta = 7.15$ (*d*, phenyl).

Intensity ratio: 3:2:3:2:2.

^{13}C–NMR (CD_2Cl_2): $\delta = 23.37, 26.81, 37.63, 45.25, 55.47, 113.83, 128.32, 141.54, 157.68$.

2. Synthesis of compound (b) BKDE

The first reaction step is the same as described in (a) using ortho-cresol instead of phenol. The yield was 80%; mp 182 °C.

Using a procedure of Brown,[51] 14.8 g 1,1-di(parahadroxyphenyl, metamethyl)-cyclohexane in dry tetrahydrofurane (THF) was slowly added to 22.75 g of a dispersion of 20% KH in paraffine in 30 ml dry THF under nitrogen atmosphere. After the H_2 evolution has stopped the salt-containing solution was pressed through a two-pointed needle using nitrogen gas. 1.5 mol of methyliodide to each hydroxy group was added in substance with a syringe through a septum and the mixture was refluxed for two days. Butanol and a solution of ammonia in methanol was added. The precipitate was filtered off and the solution was evaporated under reduced pressure. Recrystallization from methanol gives the product in a 85% yield. Further purification was done using the MPLC technique to render the product with a purity of 99.6% according to HPLC analysis; mp 73 °C.

Elementary analysis: $C_{22}H_{28}O_2$, $M = 324.44$ g/mol.

Calc.: C, 81.44; H, 8.70.

Found: C, 81.57; H, 8.71.

^{1}H–NMR (CD_2Cl_2): $\delta = 1.51$ (*m*, cyclohexyl), $\delta = 2.17$ (*s*, phenyl-CH_3), $\delta = 2.20$ (*m*, cyclohexyl), $\delta = 3.78$ (*s*, O–CH_3), $\delta = 6.40$ (*d*, phenyl), $\delta = 7.07$ (*d*, phenyl).

Intensity ratio: 3:3:2:3:1:2.

^{13}C–NMR (CD_2Cl_2): $\delta = 16.65, 23.48, 26.90, 37.62, 45.02, 55.63, 109.97, 125.51, 126.29, 129.64, 141.24, 155.86$.

We used the following apparatus: Bruker 400 MHz NMR spectrometer, Labomatic MPLC system, Perkin–Elmer DSC 7 calorimetry-analyzer, HPLC system with Waters UV detector and Merck columns.

Materials: Solvents (pro analysi Merck Schuchardt, Fluka) were thoroughly dried over sodium wire (when appropriate) and redistilled under N_2 prior to use. Cyclohexanone, phenol, ortho-cresol, dimethylsulfate, kaliumhydride 20% in paraffine, and methyliodide (p.a. Fluka) were used without further purification. The ortho-terphenyl (p.a. Merck Schuchardt) was also used without further purification.

[1] B. J. Berne and R. Pecora, Dynamic Light Scattering (Wiley, New York, 1976).

[2] E.g., D. Hwang and C. Cohen, Macromolecules **17**, 2880 (1984).

[3] M. G. Brereton, E. W. Fischer, G. Fytas, and U. Murschall, J. Chem. Phys. **86**, 174 (1987).

[4] J. Kanetakis and G. Fytas, Macromolecules **22**, 3452 (1989).

[5] M. Antonietti, J. Coutandin, R. Grütter, and H. Sillescu, Macromolecules **17**, 298 (1984).

[6] H. Lee, A. M. Jamieson, and R. Simha, J. Macromol. Sci. Phys. **B18**, 649 (1980).

[7] D. J. Coumou and E. L. Mackor, Trans. Faraday Soc. **60**, 1726 (1964).

[8] G. Delmas and R. Purves, J. Chem. Soc. Faraday Trans. 2 **71**, 1828 (1975).

[9] R. K. Bullough; Proc. R. Soc. London, Ser. A **275**, 271 (1963).

[10] Y. Sicotte, J. Chem. Phys. **61**, 1086 (1964).

[11] K. Binder, H. L. Frisch, and J. Jäckle, J. Chem. Phys. **85**, 1505 (1986).

[12] G. Fytas, Th. Dorfmüller, Y. H. Lin, and B. Chu, Macromolecules **14**, 1088 (1981).

[13] G. Fytas, Th. Dorfmüller, and B. Chu, J. Poly. Sci., Polym. Phys. Ed. **22**, 1471 (1984).

[14] G. Floudas, G. Fytas, and K. C. Ngai, Macromolecules **23**, 1104 (1990).

[15] M. Eisele and W. Burchard, Macromolecules **17**, 1636 (1986).

[16] M. Wenzel, W. Burchard, and K. Schätzel, Polymer **27**, 195 (1980).

[17] W. Brown, Macromolecules **18**, 1719 (1985).

[18] M. Schmidt, Makromol. Chem. Rapid Commun. **10**, 89 (1989).

[19] M. Wesselmann, Ph.D. thesis, University of Mainz (1989).

[20] B. Momper, G. Meier, and E. W. Fischer (unpublished).

[21] E. W. Fischer, Ch. Becker, J. U. Hagenah, and G. Meier, Colloid Polym. Sci. **80**, 198 (1989).

[22] M. Kerker, *The Scattering of Light* (Academic, New York, 1969), p. 504.

[23] N. Davidson, *Statistical Mechanics* (McGraw-Hill New York, 1962), Chap. 14.

[24] P. Debye, H. R. Anderson, and H. Brumberger, J. Appl. Phys. **28**, 679 (1957).

[25] R. N. Harward, *The Physics of Glassy Polymers* (Applied Science Publishers, Englewood Cliffs, NJ, 1973).

[26] C. H. Wang and E. W. Fischer, J. Chem. Phys. **82**, 632 (1985).

[27] G. Meier, J. U. Hagenah, C. H. Wang, G. Fytas, and E. W. Fischer, Polymer **28**, 1640 (1987).

[28] D. Boese, B. Momper, G. Meier, F. Kremer, J. U. Hagenah, and E. W. Fischer, Macromolecules **22**, 4416 (1989).

[29] J. P. Kratohvil, G. Dezelic, and M. Kerker, J. Polym. Sci. **57**, 59 (1962).

[30] F. Bueche, *Physical Properties of Polymers* (Interscience, New York, 1962).
[31] C. A. Angell, in *Relaxations in Complex Systems*, edited by K. L. Ngai and G. B. Wright (Naval. Res. Lab., Washington, DC, 1985).
[32] J. U. Hagenah, Ph.D. thesis, University of Mainz (1988).
[33] R. J. Greet and D. Turnbull, J. Chem. Phys. **46**, 1247 (1967).
[34] G. Fytas, C. W. Wang, D. Lilge, and Th. Dorfmüller, J. Chem. Phys. **75**, 4247 (1981).
[35] C. H. Wang, G. Fytas, D. Lilge, and Th. Dorfmüller, Macromolecules **14**, 1362 (1981).
[36] G. D. Patterson, Adv. Poly. Sci. **48**, 125 (1983).
[37] G. Meier, G. Fytas, and Th. Dorfmüller; Macromolecules **17**, 957 (1984).
[38] J. U. Hagenah, G. Meier, G. Fytas, and E. W. Fischer, Polymer J. **19**, 441 (1987).
[39] H. Krug, Ph.D. thesis, University of Mainz (1990).
[40] M. J. Brekner, H. A. Schneider, and H. J. Cantow, Polymer **29**, 78 (1980).
[41] K. L. Ngai, Comments Solid State Phys. **9**, 171 (1979).
[42] P. Debye and A. M. Bueche, J. Appl. Phys. **20**, 518 (1949).
[43] G. Ross, Opt. Acta **15/5**, 451 (1968).
[44] W. Thönnes; Ph.D. thesis, University of Mainz (1990).
[45] E.g., R. D. Mountain, J. Res. Natl. Bur. Stand. **70A**, 207 (1960).
[46] J. E. Frenkel, *Kinetische Theorie der Flüssigkeiten* (DVW, Berlin, 1957).
[47] A. R. Ubbelohde, *The Molten State of Matter* (Wiley, New York, 1978), Chap. 13.
[48] E. W. Fischer, G. R. Strobl, M. Dettenmaier, M. Stamm, and O. Steidle; Faraday Discuss. Chem. Soc. **68**, 26 (1979).
[49] H. Schnell, Polymer Reviews 9, (Interscience/Wiley, New York, 1964).
[50] W. F. Christopher and D. W. Fox, *Polycarbonate* (Reinhold New York, 1962).
[51] Ch. A. Brown, Synthesis **6**, 427 (1974).